Available online at www.sciencedirect.com
ScienceDirect
Journal of Photochemistry and Photobiology A: Chemistry 191 (2007) 51–58
Journal of Photochemistry and Photobiology A:Chemistry
www.elsevier.com/locate/jphotochem

Enhanced solid-state fluorescence in the oxadiazole-based excited-state intramolecular proton-transfer (ESIPT) material: Synthesis, optical property, and crystal structure

Jangwon Seo [a], Sehoon Kim [a], Young-Shin Lee [b], Oh-Hoon Kwon [b], Kang Hyun Park [b], Soo Young Choi [b], Young Keun Chung [b], Du-Jeon Jang [b], Soo Young Park [a,*]

[a] *Organic Nano-Photonics Laboratory, School of Materials Science & Engineering, Seoul National University, Seoul 151-744, Republic of Korea*
[b] *School of Chemistry, Seoul National University, Seoul 151-747, Republic of Korea*

Received 27 December 2006; received in revised form 13 March 2007; accepted 4 April 2007
Available online 7 April 2007

Abstract

We report highly fluorescent oxadiazole-based excited-state intramolecular proton-transfer (ESIPT) material, 2,5-bis-[5-(4-*tert*-butyl-phenyl)-[1,3,4]oxadiazol-2-yl]-phenol (**SOX**) in solid state film ($\Phi_f = 0.47$) as well as in solution ($\Phi_f = 0.40$). From the single crystal X-ray crystallography, a molecular geometry of **SOX** was found to be nearly planar due to the strong intramolecular hydrogen-bond between the hydroxyl and oxadiazole groups to give rise to the virtually single keto fluorescence. In view of the molecular arrangement, a specific dimer interaction caused by a Coulomb attraction in the **SOX** crystal was most likely associated with a sliding-away stacking, which contributed to the intense solid-state fluorescence. On the other hand, 2,5-bis-[5-(4-*tert*-butyl-phenyl)-[1,3,4]oxadiazol-2-yl]-benzene-1,4-diol (**DOX**) with dual ESIPT sites but otherwise the same as **SOX** showed a significantly red-shifted orange emission ($\lambda_{em} = 573$ nm) of keto tautomer relative to the bluish-green emission ($\lambda_{em} = 486$ nm) of **SOX** in chloroform. Similarly, the fluorescence emission of **DOX** in solid-state film ($\Phi_f = 0.13$) was highly enhanced from that in solution ($\Phi_f = 0.02$). Interestingly, **SOX** and **DOX** showed well-defined room-temperature phosphorescence. Kinetic studies on the ESIPT keto fluorescence as well as the phosphorescence were investigated using picosecond laser experiments.

Keywords: Excited-state intramolecular proton-transfer (ESIPT); Oxadiazole; Enhanced solid-state fluorescence; Room-temperature phosphorescence

1. Introduction

Excited-state intramolecular proton transfer (ESIPT) is a photo-induced prototropy between the enol (E) and keto (K) forms of specific organic molecule possessing intramolecular hydrogen (H)-bond. In the ground state, typical ESIPT molecules preferentially adopt enol (E) form, which is better stabilized by the intramolecular hydrogen-bonding. Upon photoexcitation, however, fast proton transfer reaction from the excited enol (E^*) occurs to give the excited keto (K^*) tautomer in a subpicosecond time scale. After decaying to the ground state, keto (K) form reverts to the original enol form via reverse proton transfer. Different absorbing ($E \rightarrow E^*$) and emitting ($K \rightarrow K^*$) molecular species in this ESIPT cycle normally result in the total exclusion of self-absorption and the large Stokes'-shifted keto emission [1,2]. Therefore, such a unique and beneficial four-level photophysical scheme has been exploited for various photonic applications [2–5].

Aiming at the high performance organic light-emitting diodes (OLED) as well as the solid-state lasers, higher values of solid-state fluorescence quantum yields with suppressed concentration quenching are basically demanded [6]. Recently, ESIPT-active oxadiazole derivative, namely, 2-(2-hydroxyphenyl)-5-phenyl-1,3,4-oxadiazole (HOXD) [7–9] has drawn a special attention as a blue emitter for OLED device due to its intense photoluminescence (PL) combining room-temperature phosphorescence and fluorescence [10]. It is also noteworthy that the 1,3,4-oxadiazole unit in HOXD provided high electron affinity as well as the thermal and chemical stabilities [11–14]. However, an intrinsic fluorescence quantum yield ($\Phi_f = 0.01$ in toluene) [9] of HOXD

* Corresponding author. Tel.: +82 2 880 8327; fax: +82 2 886 8331.
E-mail address: parksy@snu.ac.kr (S.Y. Park).

1010-6030/$ – see front matter © 2007 Elsevier B.V. All rights reserved.
doi:10.1016/j.jphotochem.2007.04.003

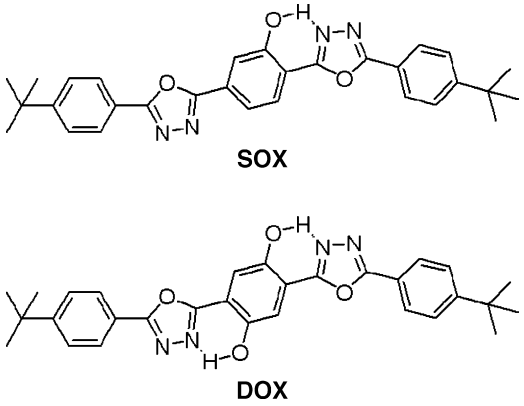

Chart 1. Molecular structures of **SOX** and **DOX** (dotted line represents intramolecular hydrogen bond).

in solution is rather small, although the solid-state photoluminescence and electroluminescence of it [10] was only qualitatively claimed to be 'intense' without any explicit quantum yield values. Therefore, a better understanding of the different PL quantum yields in solution and solid state together with the existence of room-temperature phosphorescence in a series of oxadiazole-containing ESIPT molecules is strongly demanded.

In the present work, we report novel oxadiazole-based ESIPT dye, 2,5-bis-[5-(4-*tert*-butyl-phenyl)-[1,3,4]oxadiazol-2-yl]-phenol (**SOX**) (see Chart 1) which shows strong bluish-green fluorescence in solid state ($\Phi_f = 0.47$) as well as in solution ($\Phi_f = 0.40$). As a structural analogue, 2,5-bis-[5-(4-*tert*-butyl-phenyl)-[1,3,4]oxadiazol-2-yl]-benzene-1,4-diol (**DOX**) [14c,15] with an additional hydroxyl group to **SOX** effecting a red-shifted keto fluorescence was also synthesized. In order to elucidate the photophysical processes in ESIPT molecules, the kinetic studies on fluorescence and phosphorescence were carried out by picosecond laser experiments. To understand the higher fluorescence quantum efficiencies of **SOX** and **DOX** in the solid state than those in solution, structural analyses of their single crystals were carried out and correlated with their photophysical properties.

2. Results and discussion

SOX and **DOX** were prepared via the synthetic route depicted in Scheme 1. The oxadiazole rings were formed by the reaction of **1** or **2** with 4-*tert*-butyl-benzoic acid hydrazide, and subsequent dehydrocyclization in phosphorous oxychloride ($POCl_3$). Finally, the hydroxyl group was generated by dealkylation in the presence of boron tribromide (BBr_3) in good yield. The molecular structures were identified through ^1H NMR, GC–MS and elemental analysis. The singlet protons at 10.48 ppm and 9.91 ppm from ^1H NMR accounted for a significant intramolecular H-bonding of hydroxyl proton with nitrogen atom of 1,3,4-oxadiazole in the ground state of **SOX** and **DOX**, respectively [16]. It was also noted that **SOX** and **DOX** possessed a good thermal stability: 5% weight loss was observed at the temperature higher than 350 °C (see Supplementary data).

Fig. 1 shows absorption and fluorescence emission spectra of **3**, **4**, **SOX** and **DOX** in chloroform solution. It is clearly noted

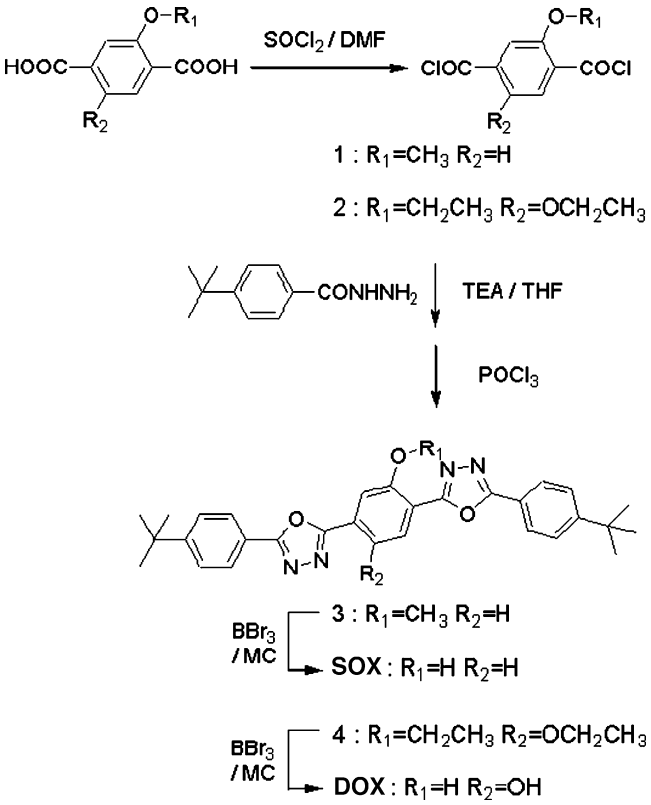

Scheme 1. Synthetic routes of **SOX** and **DOX**.

that the longest wavelength absorption bands of **SOX** and **DOX** (359 nm and 394 nm) are 20–30 nm red-shifted from those of **3** and **4** (341 nm and 365 nm) with alkoxy groups, indicating that the hydroxyl group provides extended planarity attributed to an intramolecular H-bond. For both **SOX** and **DOX**, dual emissions were observed in chloroform solution, of which the one with larger Stokes' shift was predominant relative to the normal emission with negligible intensity. Normal emissions in **3** (390 nm) and **4** (407 nm), which served as non-ESIPT models of **SOX** and **DOX** due to lack of a hydroxyl proton, were observed at the similar spectral position of normal emissions in **SOX** and **DOX**, respectively. Consequently, the large Stokes' shifted emissions could be unambiguously assigned to the keto emissions resulting from ESIPT, which exhibit bluish-green color (486 nm) and orange color (573 nm) in **SOX** and **DOX**, respectively. The spectral difference (about 90 nm) between their keto emissions looks quite large, considering that the molecular structures of **SOX** and **DOX** are identical except for the additional hydroxyl group in **DOX**. However, the individual Stokes' shifts of them, which are 0.90 eV and 0.98 eV, indicate no large difference between them. Actually, a large spectral difference in the keto emissions of **SOX** and **DOX** is mainly attributed to the similar amount of red-shift in their enol absorption bands provided by the electron donating mesomeric effect of additional hydroxyl group in **DOX**. That is, this effect is specifically due to the raised HOMO energy level from 6.1 eV of **SOX** to 5.8 eV of **DOX** at the similar LUMO levels of **SOX** (2.8 eV) and **DOX** (2.9 eV) [17]. Considering all together, ESIPT in **DOX** seems to involve single-proton transfer like in **SOX** and thus the possibility of double-proton trans-

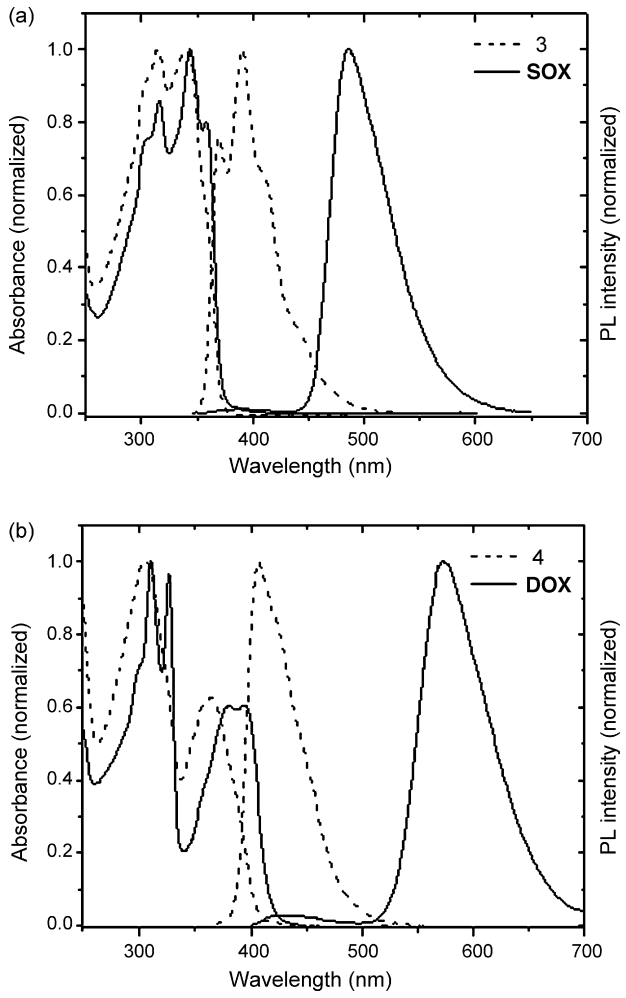

Fig. 1. Absorption and fluorescence emission spectra of (a) **3** and **SOX**, and (b) **4** and **DOX** in chloroform solution (10^{-5} M), respectively.

fer is excluded like in 2,5-bis(2′-benzoxazolyl)hydroquinone (BBHQ) [18].

The fluorescence kinetic profiles of **SOX** in chloroform solution are displayed in Fig. 2, which were monitored at 380 nm and 550 nm as probe wavelength for enol and keto emissions, respectively. From the best fitting results of the fluorescence rise and decay of **SOX** data, the lifetimes were determined and compiled in Table 1. Compared to the absence of rise component in the enol emission detected at 380 nm that with a time constant of less than 10 ps was observed at the probe wavelength of 550 nm. This typical rise component of keto emission, which also correlates well with the shorter decay component (<10 ps, see Table 1) of the photoexcited enol, evidences the formation of keto component via ESIPT process from the photoexcited enol [1a,5a]. Similarly, in case of **DOX**, the rise component for proton transfer was also detected from kinetic profile probed at 650 nm. Fluorescence decay kinetics of the keto tautomers could be well fitted by single-exponential decays, as included in Table 1. It was noted that the lifetime of 3900 ps in **SOX** was much longer than that of 650 ps in **DOX**. Correspondingly, the fluorescence quantum yield (Φ_f) of **SOX** in chloroform was as high as 0.40, but that of **DOX** was relatively low as 0.02. As shown in Fig. 1, additional hydroxyl group substituted at the *para*-position of proton donor species has brought about a significant red-shift of absorption band in keto tautomer relative to **SOX**. This may be related to a rather lower fluorescence intensity of **DOX**, most likely due to the energy-gap law [18c,19], which means that the internal conversion rate increases and Φ_f decreases as energy difference between two states (mostly, S0 → S1 transition energy) decreases. Alternatively, additional hydroxyl group as electron donor most likely resulted in a decrease of acidity in the phenolic OH as proton donor and thus weakening an intramolecular H-bond [20], as manifested by the relatively larger intensity ratio of normal (enol) to keto emission in **DOX** than that in **SOX**. Moreover, it was supported by the slightly longer distance (1.90 Å) of intramolecular H-bond in **DOX** than that (1.66 Å) in **SOX** (*vide infra* for X-ray crystallographic analysis). In particular, for **DOX**, fluorescence decrease in solution may occur to the higher degree than that for **SOX**, considering a presence of additional OH stretching mode (due to the two hydroxyl groups) as radiationless deactivation route [21].

Table 1
Fluorescence quantum yields and lifetimes of **SOX** and **DOX** together with the phosphorescence data

	Quantum yield, Φ_f	λ_{em}	Rise	Decay
SOX	0.40[a]	380	Fast	≤10,920 ps
		550	≤10 ps	3900 ps
		490		36 μs[c]
DOX	0.02[b]	450	Fast	≤10,650 ps
		650	≤10 ps	650 ps
		510		5.6 μs[c]

[a] 3,4,9,10-Perylenetetracarboxylic dianhydride in 0.1 M K_2CO_3 as reference.
[b] Rhodamine 6G in EtOH as reference.
[c] Phosphorescence lifetime.

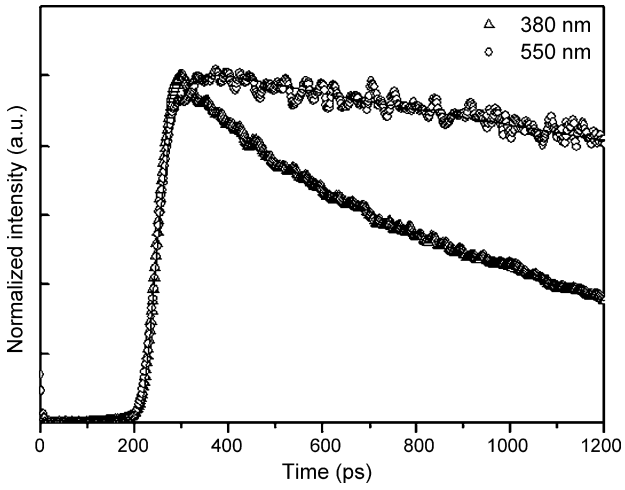

Fig. 2. Fluorescence kinetic profiles of **SOX** in chloroform solution (10^{-5} M), observed at two probe wavelengths of 380 nm (Δ) and 550 nm (◯). The solid curves are the results of fitting analyses.

Fig. 3 shows the phosphorescence spectra of **SOX** and **DOX** at room temperature under argon atmosphere [22]. The kinetic profiles exhibited single-exponential decay with the lifetime of 36 μs and 5.6 μs for **SOX** and **DOX**, respectively. This observation of room-temperature phosphorescence in the

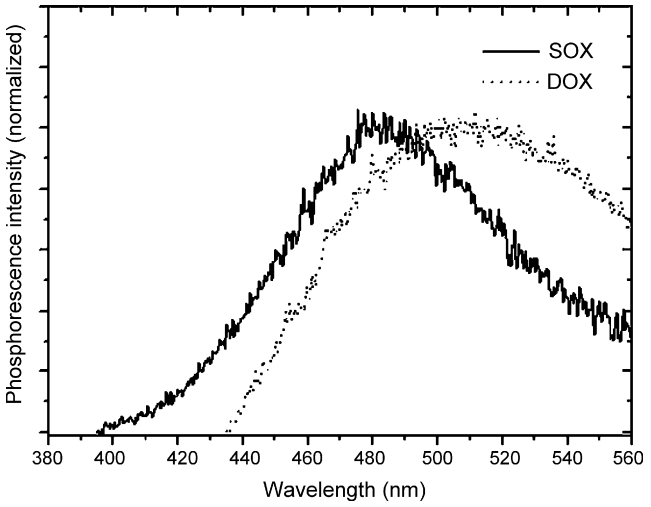

Fig. 3. Phosphorescence spectra of **SOX** and **DOX** in chloroform solution ($\sim 10^{-5}$ M and $\sim 10^{-4}$ M, respectively). The experiment was carried out at room temperature with samples substituted by and blanketed under argon atmosphere.

oxadiazole-based ESIPT molecules is consistent with the broad phosphorescence band of HOXD reported earlier [10] and thus provides the general evidences. For most of the luminescent organic compounds, only the singlet-excited state is emissive at room temperature, resulting in the limited efficiency in OLED, in principle. Therefore, the development of fluorescent organic materials with room-temperature phosphorescence is an important challenge. This is relevant to the substantial enhancement in the OLED device efficiency by utilizing emissions from both the singlet and the triplet states [23]. Phosphorescence bands of **SOX** and **DOX**, which are centered at around 480 nm and 505 nm, are located at and integrated into the higher energy spectral position of the corresponding ESIPT keto fluorescence bands, as seen in Fig. 1. Based on the previous literatures [10,24], it is most likely that the phosphorescence spectra originate from the excited triplet state of enol rather than that of keto tautomer.

To gain a deeper insight into the fluorescence property in the solid state demanded for device application, Φ_f of **SOX** and **DOX** in the solid-state film were measured to be 0.47 and 0.13, respectively [25]. It is noteworthy that the fluorescence quantum yields in the film were significantly enhanced compared to those of 0.40 and 0.02 in solution (chloroform), respectively. Such a distinct enhancement in the solid is, most probably, due to the reduced internal conversion caused by the limited vibrational relaxation. Limited internal rotation in the solid state is similarly effective: H-bonded conformer was energetically preferred to increase total emission, including the ESIPT fluorescence [10,26].

Table 2
Crystallographic data of **SOX** and **DOX**

	SOX	**DOX**
Empirical formula	$C_{30}H_{30}N_4O_3$	$C_{30}H_{30}N_4O_4$
Fw	494.58	510.58
Crystal system	Triclinic	Triclinic
Space group	*P*-1	*P*-1
a (Å)	9.745(5)	6.1363(3)
b (Å)	11.274(5)	9.8113(7)
c (Å)	12.794(5)	10.9340(8)
α (°)	74.688(5)	79.933(3)
β (°)	80.500(5)	87.319(4)
γ (°)	77.101(5)	87.682(4)
V (Å^3)	1313.1(10)	647.09(14)
Z	2	1
d (calcd.) (Mg/m^3)	1.251	1.310
θ range (°)	2.16–27.50	3.07–27.46
Total number of data collected	8853	4028
Number of unique data	5961	2920
Number of parameters refined	342	232
*R*1 ($I > \sigma(I)$)	0.0817	0.0538
*wR*2 ($I > \sigma(I)$)	0.2201	0.1279
GOF	1.017	1.022

In addition, the fluorescence behavior in solid state must be closely correlated with molecular geometry and intermolecular packing arrangement. In order to correlate the fluorescence behavior with the molecular packing structure, single crystals of **SOX** and **DOX** were prepared from ethylacetate and dichloromethane solution, respectively. The crystallographic data of **SOX** and **DOX** are given in Table 2. As shown in Fig. 4, **SOX** has a nearly planar structure at central three rings (central phenol ring and two adjacent oxadiazole rings) with only a slight torsion (less than 4.9°) relative to each other. As expected, the intramolecular H-bonding between hydrogen atom of hydroxyl group and nitrogen atom of oxadiazole group is apparent with its distance of 1.66 Å, which reveals an efficient geometry for ESIPT process excluding the formation of rotamer [1a] giving rise to a normal emission. On the other hand, two peripheral *tert*-butyl benzene rings were slightly twisted with torsional angles ranging between 15.1° and 17.2° relative to the oxadiazole rings.

Fig. 5 shows top view (a) and side views (b and c) of coupled **SOX** molecules in a single crystal which are oriented antiparallel from each other along the long axis of molecules. They are not perfectly superimposed in a face-to-face fashion between aryl groups like in excimer, but are both laterally and axially trans-

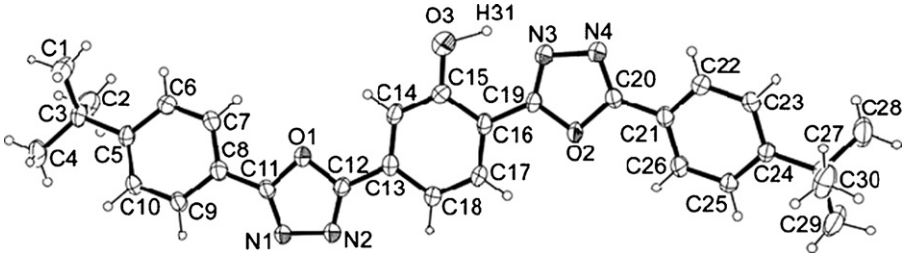

Fig. 4. ORTEP drawing of **SOX** with 30% probability ellipsoids.

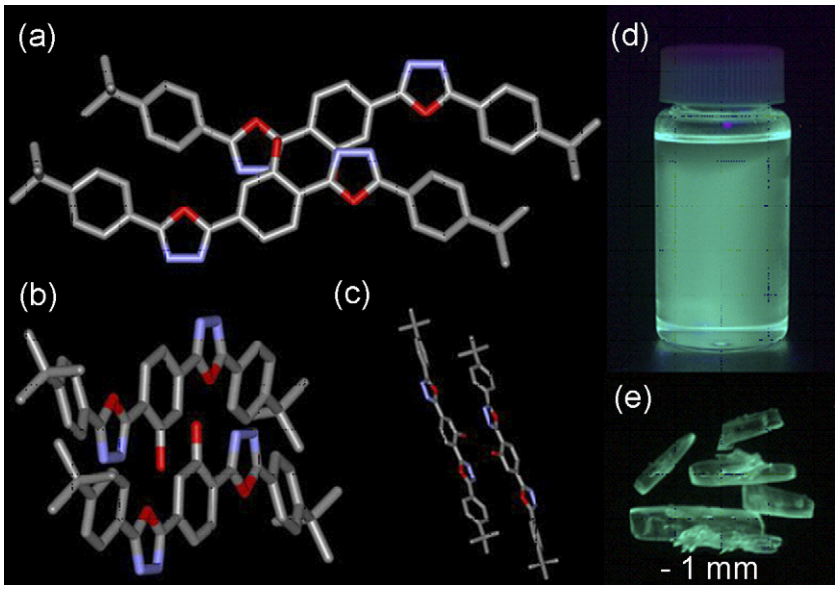

Fig. 5. (a) Top view and (b and c) side views of two neighboring molecules in single crystal of **SOX**. Fluorescence images (d) in chloroform solution and (e) in single crystal (excitation with 365 nm hand-held UV lamp).

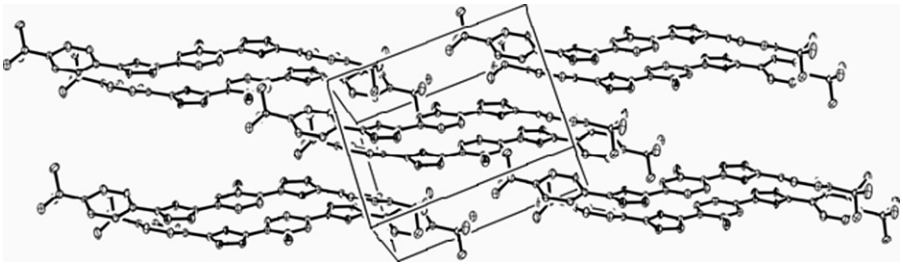

Fig. 6. Packing arrangement of **SOX** molecules in a single crystal.

lated along the long axis of one molecule. Such a 'sliding-away stacking' (a kind of J-aggregate pattern) in **SOX** is considered to suppress a drastic concentration quenching and to keep the intense fluorescence emission in the solid state. Similar observations as a strong and enhanced solid-state fluorescence were already reported in J-type aggregates like CN-MBE [6a] and also in the molecules with limited twist like a silole derivative [6b] and imidazole-based dye (HPI) [6c]. As shown in Fig. 5e, strong keto fluorescence from the single crystal could be readily observed much like that in solution (chloroform) shown in Fig. 5d. Top view in Fig. 5a clearly displays that two imaginary rings (H31–O3–C15–C16–C19–N3) formed by intramolecular H-bond (in front as well as in rear molecule) were overlapped with a distance of ca. 3.3 Å. That is, C15 (0.179) [27] of the central phenol ring in the front molecule, which is positively charged, is positioned in an approximately vertical line at N3 (−0.137) [27] of the oxadiazole ring in the rear molecule, bearing a negative charge. Similarly, O3 (−0.246) [27] in the front molecule is located above C19 (0.057) [27] in the rear molecule. As a result, such a specific Coulomb attraction [28] between two neighboring molecules plays a key role in a unique dimeric arrangement in crystal packing, as shown in Fig. 6.

Such a specific interaction in **SOX** worked similarly for the packing arrangement of **DOX** crystal, as shown in Figs. S3 and S4 (Supplementary data). A consecutive sliding-away stacking along the specific aligning direction (symbolized by A axis of unit cell) was found, probably due to an intermolecular Coulomb attraction caused by symmetric molecular structure of **DOX** (Fig. S2). In view of the fluorescence behavior, this kind of molecular stacking has resulted in a much brighter keto emission in crystal compared to the weak emission in solution (Fig. S4).

3. Conclusions

Two fluorescent ESIPT molecules, **SOX** and **DOX**, containing photoactive 1,3,4-oxadiazoles together with one and two intramolecular H-bonding sites were synthesized. **SOX** showed an intense keto emission with bluish-green color in solid state ($\Phi_f = 0.47$ in PS film) as well as in solution ($\Phi_f = 0.40$ in chloroform). Similarly, **DOX** exhibited highly enhanced orange keto emission in the solid film ($\Phi_f = 0.13$) compared to that ($\Phi_f = 0.02$) in solution. For both **SOX** and **DOX**, room-temperature phosphorescence was observed under argon atmosphere. Single crystal X-ray crystallography suggested that sliding-away stacking (J-type aggregate packing) of **SOX** and **DOX** molecules were responsible for the enhanced fluorescence emission in the solid-state. Based

on the unique properties of enhanced emission and room-temperature phosphorescence, **SOX** and **DOX** hold strong potential for the solid-state photonic applications like OLED and solid-state laser. One specific application of **SOX–DOX** combination for white OLED fabrication was published separately [29].

4. Experimental

4.1. Materials

4-*tert*-Butyl-benzoic acid hydrazide and 2,5-diethoxy-terephthalic acid were prepared according to the literature procedures [30,31]. All the other chemicals were purchased commercially, and used without further purification.

4.1.1. 2,5-Bis-[5-(4-tert-butyl-phenyl)-[1,3,4]oxadiazol-2-yl]-methoxy-benzene (*3*)

A mixture of 2-methoxy-terephthalic acid (1.50 g, 7.65 mmol), DMF (two drops), and thionyl chloride (5 ml) was refluxed for 4 h. After cooling, excess thionyl chloride was distilled out. The residual mixture was dissolved in THF (40 ml), and then, was added in a dropwise manner to a solution of 4-*tert*-butyl-benzoic acid hydrazide (3.10 g, 16.12 mmol), triethylamine (6.4 ml) and THF (40 ml). The reaction mixture was stirred for 6 h at room temperature. After the solvent was removed under vacuum, the residue was poured into water. The precipitate was filtered, washed with water and ethanol, and dried. A mixture of the dried solid and $POCl_3$ (10 ml) was refluxed overnight. After cooling, the resulting mixture was poured slowly into ice water and neutralized with aqueous NaOH solution. The crude product was collected by filtration and purified by recrystallization from ethanol/chloroform to afford 1.80 g as white crystals ($Y = 46\%$). Mp = 290 °C; ^{1}H NMR ($CDCl_3$, ppm) 8.22 (d, $J = 8.1$ Hz, 1H), 8.10 (d, $J = 8.4$ Hz, 2H), 8.09 (d, $J = 8.4$ Hz, 2H), 7.89 (d, $J = 1.1$ Hz, 1H), 7.83 (dd, $J = 8.1$, 1.5 Hz, 1H), 7.59 (d, $J = 8.4$ Hz, 2H), 7.57 (d, $J = 8.4$ Hz, 2H), 4.14 (s, 3H), 1.39 (s, 18H); *m/z* (EI) calcd. for $C_{31}H_{32}N_4O_3$, 508.61; found 508; Anal. Calcd. for $C_{31}H_{32}N_4O_3$: C, 73.21; H, 6.34; N, 11.02. Found: C, 72.87; H, 6.49; N, 11.32.

4.1.2. 2,5-Bis-[5-(4-tert-butyl-phenyl)-[1,3,4]oxadiazol-2-yl]-1,4-diethoxy-benzene (*4*)

According to the same procedure as above, **4** was prepared using 2,5-diethoxy-terephthalic acid (0.30 g, 1.18 mmol) and 4-*tert*-butyl-benzoic acid hydrazide (0.50 g, 2.60 mmol). The crude product was purified by recrystallization from ethanol/chloroform to afford 0.52 g as pale yellow crystals ($Y = 78\%$). Mp = 285 °C; ^{1}H NMR ($CDCl_3$, ppm) 8.08 (d, $J = 8.7$ Hz, 4H), 7.84 (s, 2H), 7.57 (d, $J = 8.6$ Hz, 4H), 4.28 (q, 4H), 1.58 (t, 6H), 1.38 (s, 18H); *m/z* (EI) calcd. for $C_{34}H_{38}N_4O_4$, 566.69; found 566; Anal. Calcd. for $C_{34}H_{38}N_4O_4$: C, 72.06; H, 6.76; N, 9.89. Found: C, 72.00; H, 6.74; N, 9.95.

4.1.3. 2,5-Bis-[5-(4-tert-butyl-phenyl)-[1,3,4]oxadiazol-2-yl]-phenol (*SOX*)

To a solution of **3** (1.0 g, 1.97 mmol) and dichloromethane (30 ml), boron tribromide (2.6 ml, 27.5 mmol) was added dropwise at −78 °C. After 30 min, the reaction mixture was stirred for 6 h at room temperature. The reaction mixture was slowly poured into ice water and neutralized with aqueous sodium bicarbonate solution. After dichloromethane was removed under vacuum, the precipitate was collected by filtration and washed with water. The crude product was purified by recrystallization from ethanol/chloroform to afford 0.77 g as white crystals ($Y = 79\%$). Mp = 278 °C; ^{1}H NMR ($CDCl_3$, ppm) 10.48 (s, 1H), 8.08 (d, $J = 8.2$ Hz, 2H), 8.07 (d, $J = 8.2$ Hz, 2H), 8.02 (d, $J = 8.8$ Hz, 1H), 7.85–7.87 (m, 2H), 7.58 (d, $J = 8.4$ Hz, 2H), 7.56 (d, $J = 8.3$ Hz, 2H), 1.37 (s, 18H); *m/z* (EI) calcd. for $C_{30}H_{30}N_4O_3$, 494.58; found 494; Anal. Calcd. for $C_{30}H_{30}N_4O_3$: C, 72.85; H, 6.11; N, 11.33. Found: C, 72.49; H, 6.12; N, 11.23.

4.1.4. 2,5-Bis-[5-(4-tert-butyl-phenyl)-[1,3,4]oxadiazol-2-yl]-benzene-1,4-diol (*DOX*)

According to the same procedure as above, **DOX** was prepared from **4** (0.31 g, 0.55 mmol) and boron tribromide (0.7 ml, 7.66 mmol). The crude product was purified by recrystallization from ethanol/chloroform to afford 0.25 g as pale yellow powder ($Y = 90\%$). Mp was not observed up to 300 °C; ^{1}H NMR ($CDCl_3$, ppm) 9.91 (s, 2H), 8.10 (d, $J = 8.7$ Hz, 4H), 7.67 (s, 2H), 7.60 (d, $J = 8.6$ Hz, 4H), 1.39 (s, 18H); *m/z* (EI) calcd. for $C_{30}H_{30}N_4O_4$, 510.58, found 510; Anal. Calcd. for $C_{30}H_{30}N_4O_4$: C, 70.57; H, 5.92; N, 10.97. Found: C, 70.34; H, 6.03; N, 10.87.

5. Measurements

5.1. General measurements

^{1}H NMR spectra were recorded on a JEOL JNM-LA300 (300 MHz) in $CDCl_3$ solutions. Mass spectra were measured on a JMS AX505WA by EI mode. Elemental analysis was carried out with CE instrument EA1110. Thermogravimetric analysis (TGA) was performed with TA instrument TA5000/TGA 2950 at a heating rate of 10 °C/min under a nitrogen flow. Differential scanning calorimetry (DSC) was measured on Perkin-Elmer DSC7 at a heating rate of 20 °C/min. UV–vis absorption spectra were recorded on Shimadzu UV-2101PC. Emission spectra were obtained using a home-built spectrometer, which consisted of a 75 W Xe lamp (Acton Research, XS 432), two monochromators (Acton Research, Spectrapro 150 and 300 mm), and a photomultiplier tube (Acton Research, PD 438). Fluorescence quantum yields (Φ_f) in chloroform solution were relatively determined by comparison with 3,4,9,10-perylenetetracarboxylic dianhydride in 0.1 M K_2CO_3 and Rhodamine 6G in ethanol as the references for **SOX** and **DOX**, respectively [32]. Φ_f in film was measured using a 6 in. integrating sphere (Labsphere, 3P-GPS-060-SF) equipped with a 325 nm CW He–Cd laser (Omnichrome, Series 56) and a PMT detector (Hamamatsu, PD471) attached to a monochromator (Acton Research, Spectrapro-300i). The detailed analytic procedure to obtain Φ_f in film has been described elsewhere [33].

Fluorescence lifetime measurement. Fluorescence kinetic profiles, excited with Raman-shifted 315 nm pulses of a mode-locked Nd:YAG laser (Quantel, YG701), were detected using a 10 ps streak camera (Hamamatsu, C2830). Emission wavelengths were selected by combining band-pass filters and cut-off filters. Fluorescence kinetic constants were extracted by fitting profiles to the computer-simulated exponential curves convoluted with instrumental response functions (fwhm: 25 ps).

Phosphorescence spectra and lifetime measurement. Phosphorescence spectra and decay kinetic profiles were measured using an intensified CCD (Princeton Instruments, ICCD576G) of 2 ns gating resolution, which was attached to a 0.5 m spectrometer (Acton Research, Spectrapro-500). The fourth-harmonic pulses of a Q-switched Nd:YAG laser (Quantel, Brilliant) were used to excite samples at room temperature under argon atmosphere. Kinetic constants were extracted by fitting measured kinetic profiles to computer-simulated kinetic curves.

X-ray crystallographic analysis. X-ray data for a single crystal was collected on the Enraf-Nonius CCD single crystal X-ray diffractometer at room temperature using graphite-monochromated Mo Kα radiation ($\lambda = 0.71073$ Å). The structure was solved by direct methods (SHELXS-97), and refined against all F^2 data (SHELXS-97). All non-hydrogen atoms were refined with anisotropic thermal parameters. All hydrogen atoms in **DOX** found in the Fourier map and were refined. All hydrogen atoms in **SOX** were treated as idealized contributions. Crystallographic data for **DOX** and **SOX** have been deposited with the Cambridge Crystallographic Data Centre as supplementary publication numbers of CCDC 285830 and 285831, respectively. These data can be obtained free charge via www.ccdc.cam.ac.uk/products/request/ (or from the Cambridge Crystallographic Data Centre, 12 Union Road, Cambridge CB21EZ, UK; fax: +44 1223 336 033; or deposit@ccdc.cam.ac.uk).

Acknowledgments

This work was supported by the Korea Science and Engineering Foundation (KOSEF) through the National Research Lab. Program funded by the Ministry of Science and Technology (no. 2006-032246). We are grateful for the instrumental supports from the equipment facilities of Dongwoo Finechem Co. Ltd. and OLED center-Seoul National University.

Appendix A. Supplementary data

Supplementary data associated with this article can be found, in the online version, at doi:10.1016/j.jphotochem.2007.04.003.

References

[1] (a) O.K. Abou-Zied, R. Jimenez, E.H.Z. Thompson, D.P. Millar, F.E. Romesberg, J. Phys. Chem. A 106 (2002) 3665;
(b) J. Seo, S. Kim, S.Y. Park, J. Am. Chem. Soc. 126 (2004) 11154.
[2] (a) A.U. Acuña, A. Costela, J.M. Muñoz, J. Phys. Chem. 90 (1986) 2807;
(b) R.M. Tarkka, X. Zhang, S.A. Jenekhe, J. Am. Chem. Soc. 118 (1996) 9438;
(c) S. Kim, D.W. Chang, S.Y. Park, S.C. Jeoung, D. Kim, Macromolecules 35 (2002) 6064.
[3] S. Kim, S.Y. Park, I. Yoshida, H. Kawai, T. Nagamura, J. Phys. Chem. B 106 (2002) 9291.
[4] F. Vollmer, W. Rettig, J. Photochem. Photobiol. A 95 (1996) 143.
[5] (a) D.W. Chang, S. Kim, S.Y. Park, H. Yu, D.-J. Jang, Macromolecules 33 (2000) 7223;
(b) S. Kim, D.W. Jang, S.Y. Park, K. Kim, J.-I. Jin, Bull. Kor. Chem. Soc. 22 (2001) 1407.
[6] (a) B.-K. An, S.-K. Kwon, S.-D. Jung, S.Y. Park, J. Am. Chem. Soc. 124 (2002) 14410;
(b) J. Luo, Z. Xie, J.W.Y. Lam, L. Cheng, H. Chen, C. Qiu, H.S. Kwok, X. Zhan, Y. Liu, D. Zhu, B.Z. Tang, Chem. Commun. 18 (2001) 1740;
(c) S. Park, O.-H. Kwon, S. Kim, S. Park, M.-G. Choi, M. Cha, S.Y. Park, D.-J. Jang, J. Am. Chem. Soc. 127 (2005) 10070;
(d) S.H. Lee, B.-B. Jang, Z.H. Kafafi, J. Am. Chem. Soc. 127 (2005) 9071.
[7] H. Tong, G. Zhou, L. Wang, X. Jing, F. Wang, J. Zhang, Tetrahedron Lett. 44 (2003) 131.
[8] (a) J.F. Wang, G.E. Jabbour, E.A. Mash, J. Anderson, Y. Zhang, P.A. Lee, N.R. Armstrong, N. Peyghambarian, B. Kippelen, Adv. Mater. 11 (1999) 1266;
(b) N.-X. Hu, M. Esteghamatian, S. Xie, A.-M. Popovic, B. Ong, S. Wang, Adv. Mater. 11 (1999) 1460.
[9] A.O. Doroshenko, E.A. Porokhov, A.A. Verezubova, L.M. Ptyagina, J. Phys. Org. Chem. 13 (2000) 253.
[10] (a) F. Liang, L. Wang, D. Ma, X. Jing, F. Wang, Appl. Phys. Lett. 81 (2002) 4;
(b) D. Ma, F. Liang, L. Wang, S.T. Lee, L.S. Hung, Chem. Phys. Lett. 358 (2002) 24.
[11] S.W. Kim, S.C. Shim, B.-J. Jung, H.-K. Shim, Polymer 43 (2002) 4297.
[12] X. Zhang, S.A. Jenekhe, Macromolecules 33 (2000) 2069.
[13] A.P. Kulkarni, C.J. Tonzola, A. Babel, S.A. Jenekhe, Chem. Mater. 16 (2004) 4556.
[14] (a) M. Thelakkat, H.-W. Schmidt, Polym. Adv. Technol. 9 (1998) 429;
(b) H. Tokuhisa, M. Era, T. Tsutsui, Appl. Phys. Lett. 72 (1998) 2639;
(c) Z. Peng, J. Zhang, Chem. Mater. 11 (1999) 1138.
[15] Although DOX was previously reported as the intermediate compound for synthesis of EL material, its optical property related to ESIPT has not been investigated yet.
[16] C.E.M. Carvalho, I.M. Brinn, A.V. Pinto, M.C.F.R. Pinto, J. Photochem. Photobiol. A 123 (1999) 61.
[17] Energy levels were determined by cyclic voltammetry (CV) measurement and optical spectroscopy (see Fig. S5 and Table S1 in Supplementary data).
[18] (a) S. Nagaoka, U. Nagashima, J. Phys. Chem. 94 (1990) 1425;
(b) A. Mordziński, A. Grabowska, W. Kühnle, A. Krówczyński, Chem. Phys. Lett. 101 (1983) 291;
(c) A. Mordziński, A. Grabowska, K. Teuchner, Chem. Phys. Lett. 111 (1984) 383.
[19] (a) H. Fidder, M. Rini, E.T.J. Nibbering, J. Am. Chem. Soc. 126 (2004) 3789;
(b) S. Nagaoka, A. Nakamura, U. Nagashima, J. Photochem. Photobiol. A 154 (2002) 23.
[20] (a) J. Ouyang, C. Ouyang, Y. Fujii, Y. Nakano, T. Shoda, T. Nagano, J. Heterocycl. Chem. 41 (2004) 359;
(b) A. Douhal, F. Amat-Guerri, M.P. Lillo, A.U. Acuña, J. Photochem. Photobiol. A 78 (1994) 127.
[21] (a) H. Lanig, Th. Engel, G. Käb, F.W. Schneider, Chem. Phys. Lett. 235 (1995) 58;
(b) G. Grabner, G. Köhler, G. Marconi, S. Monti, E. Venuti, J. Phys. Chem. 94 (1990) 3609.
[22] In case of samples exposed to oxygen in air, phosphorescence was not observed at room temperature.
[23] A. Köhler, J.S. Wilson, R.H. Friend, Adv. Mater. 14 (2002) 701.
[24] (a) M. Kasha, J. Heldt, D. Gormin, J. Phys. Chem. 99 (1995) 7281;
(b) A. Mordziński, K.H. Grellmann, J. Phys. Chem. 90 (1986) 5503.
[25] All three polystyrene (PS) films doped with the different amount of SOX (2, 5, and 10 wt%) showed Φ_f of 0.47. In PS film doped with DOX (5 wt%),

Φ_f was found to be 0.13. However, in case of the higher doped system, we could not try due to solubility problem of DOX.

[26] (a) C.E.M. Carvalho, A.S. Silva, I.M. Brinn, A.V. Pinto, M.C.F.R. Pinto, S. Lin, T.A. Moore, D. Gust, M. Maeder, Phys. Chem. Chem. Phys. 4 (2002) 3383;
(b) D. LeGourrierec, V. Kharlanov, R.G. Brown, W. Rettig, J. Photochem. Photobiol. A 117 (1998) 209;
(c) G. Oster, Y. Nishijima, J. Am. Chem. Soc. 78 (1956) 1581;
(d) D.L. Williams, A. Heller, J. Phys. Chem. 74 (1970) 4473.

[27] Charges (electron unit) of single molecule, which were obtained by semi-empirical calculation using HyperChem 7.0 package (HyperCube Inc., Copyright 2002) with PM3 method based on the conformation in gas phase, were denoted in parentheses.

[28] R.E. Gill, P.F. vanHutten, A. Meetsma, G. Hadziioannou, Chem. Mater. 8 (1996) 1341.

[29] S. Kim, J. Seo, H.K. Jung, J.-J. Kim, S.Y. Park, Adv. Mater. 17 (2005) 2077.

[30] D.W. Lee, K.-Y. Kwon, J.-I. Jin, Y. Park, Y.-R. Kim, I.-W. Hwang, Chem. Mater. 13 (2001) 565.

[31] G.A. Sotzing, J.R. Reynolds, A.R. Katritzky, J. Soloducho, S. Belyakov, R. Musgrave, Macromolecules 29 (1996) 1679.

[32] (a) H. Langhals, J. Karolin, L.B.-Å. Johansson, J. Chem. Soc., Faraday Trans. 94 (1998) 2919;
(b) J.R. Lakowicz, Principles of Fluorescence Spectroscopy, 2nd ed., Plenum, New York, 1999, pp. 51–53.

[33] J.C. de Mello, H.F. Wittmann, R.H. Friend, Adv. Mater. 9 (1997) 230.